Multiple Conductance States of the Light-activated Channel of *Limulus* Ventral Photoreceptors

Alteration of Conductance State during Light

EDWIN C. JOHNSON, JUAN BACIGALUPO, CECILIA VERGARA, and JOHN E. LISMAN

From the Department of Physiology, Marshall University School of Medicine, Huntington, West Virginia 25755-9340; Departamento de Biologia, Facultad de Ciencias, Universidad de Chile, Santiago, Chile; and Department of Biology, Brandeis University, Waltham, Massachusetts 02254

ABSTRACT The properties of light-dependent channels in *Limulus* ventral photoreceptors have been studied in cell-attached patches. Two sizes of single-channel events are seen during illumination. Previous work has characterized the large (40 pS) events; the goal of the current work was to characterize the small (15 pS) events and determine their relationship to the large events. The small events are activated by light rather than as a secondary result of the change in membrane voltage during light. The mean open time of the small events is 1.34 ± 0.49 ms (mean ± SD, $n = 15$), ~50% of that of the large events. The large and small events have the same reversal potential and a similar dependence of open-state probability on voltage. Evidence that these events are due to different conductance states of the same channel comes from analysis of relatively infrequent events showing a direct transition between the 15 and 40-pS levels. Furthermore, large and small events do not superpose, even at positive voltages when the probability of being open is very high, as would be predicted if the two-sized events were due to independent channels. Expression of the different conductance states is not random; during steady illumination there are alternating periods of several hundred milliseconds in which there are consecutive, sequential large events followed by periods in which there are consecutive, sequential small events. At early times during the response to a step of light, the large conductance state is preferentially expressed. At later times, there is an increase in the relative contribution of the low conductance state. These findings indicate that there is a process that changes the preferred conductance state of the channel. This alteration has functional importance in the process of light adaptation.

Address reprint requests to Dr. Edwin C. Johnson, Department of Physiology, Marshall University School of Medicine, 1542 Spring Valley Drive, Huntington, WV 25755-9340.

J. GEN. PHYSIOL. © The Rockefeller University Press · 0022-1295/91/06/1187/19 $2.00
Volume 97 June 1991 1187–1205

INTRODUCTION

Limulus photoreceptors depolarize in response to light as a result of an inward current that flows through ionic channels activated by the phototransduction cascade (Millecchia and Mauro, 1969; Wong et al., 1982; Bacigalupo and Lisman, 1983; Bacigalupo et al., 1986). The second messenger reponsible for opening the light-activated channels of invertebrate photoreceptors may be cGMP (Johnson et al., 1986; Bacigalupo et al., 1990, 1991). Previous work showed that light activates channels having a conductance of 40 pS. In addition, preliminary evidence was reported for small events present during light (Bacigalupo and Lisman, 1983; Bacigalupo et al., 1987). The main purpose of this paper is to further examine these small events. We have concluded that they are due to a different conductance state of the same channel that generates the large events, rather than due to a completely different type of channel. We have also studied the sequence of large and small events during the response to light. Such analysis reveals that the sequence is far from random. The channel cycles between modes in which the channel repeatedly opens to the same conductance state. Furthermore, there is a regulatory process that reduces the relative contribution of the high-conductance mode as the response to light proceeds. This alteration contributes to the function of light adaptation in these photoreceptors. A preliminary account of some of this work has been presented (Bacigalupo et al., 1987; Lisman et al., 1990).

MATERIALS AND METHODS

The experiments were done on ventral photoreceptors from male horseshoe crabs obtained from the Marine Biological Laboratory, Woods Hole, MA, and kept either in seawater tanks or in a moistened environment in a cold room for <10 d. Ventral nerves were removed and treated with Pronase (Calbiochem-Behring Corp., La Jolla, CA; 2% for 30–60 s) to soften connective tissue, a procedure that is standard for this preparation. Individual photoreceptors from these nerves were stripped of their surrounding connective tissue by means of a suction pipette, as described by Stern et al. (1982). All experiments were done at room temperature.

Patch pipettes (Garner Glass, Claremont, CA; no. 7052) filled with artificial seawater (in millimolar: 425 NaCl, 10 KCl, 22 $MgCl_2$, 26 $MgSO_2$, 10 $CaCl_2$, 15 Tris Cl, pH 7.8) were sealed against the light-sensitive membrane of the photoreceptors (the R-lobe membrane). Seal resistances between 5 and 100 GΩ were obtained. Unlike work using a different pipette glass (Bacigalupo et al., 1986), seals could be obtained without using the mild sonication procedure previously required. After obtaining the gigaseal, a series of depolarizing voltage steps was applied in the dark in order to determine whether channels other than the light-activated channels were present in the patch. We proceeded with an experiment only if the patch contained solely light-activated channels. Data were stored on an FM tape recorder or on a video cassette recorder through a digital interface for subsequent analysis.

For analysis, the current records were low-pass filtered using an eight-pole Bessel filter (model 902; Frequency Devices, Haverhill, MA), set at a bandwidth of half the sample frequency, normally 10–40 kHz. Data were sampled by a Digital computer system (Indec Systems, Sunnyvale, CA) or by an IBM AT compatible system (Indec Systems) and filtered with a Gaussian digital filter. The overall bandwidth of the signal indicated in the figure legends was determined by the sum of the cutoff frequencies of the components. In addition to the bessel filter, the digital Gaussian filter of the computer was normally 2.5 kHz, and the patch-clamp bandwidth was 10 kHz, resulting in a total cutoff frequency of 2.37 kHz. When using the FM

recorder, which had a very sharp cutoff at about 4 kHz, the cutoff frequency was slightly lower (2.3 kHz).

Histograms of the raw current records were constructed from digitized data. The composite cutoff frequency for these data was 2.3 kHz, giving a rise time (10–90%) of 0.15 ms. As a result of the finite bandwidth, transitions between event levels contribute to this histogram. The data were fit with a multiple Gaussian distribution using a standard Levenberg-Marquardt algorithm as implemented in pClamp 5.5.

Histograms of idealized records were constructed using an interactive detection program (Fetchan in pClamp 5.5) with a 50% detection threshold. Events were included for histogram analysis only if they were open long enough to allow the digital Gaussian filter to settle (twice the Gaussian filter rise time). Thus, events shorter than 0.5 ms were normally not included in the amplitude and open time distributions. In addition, closings shorter than 0.150 ms were ignored. For this reason, the open time distributions should technically be considered the distribution of burst times. The minimum in the double Gaussian fit of the amplitude distribution was used to determine which subset of the data was used for determining the open time distribution for the 15- and the 40-pS events. The open time was calculated as the time between two 50% threshold crossings from an event that was open long enough for the amplitude to be accurately determined (if the digital Gaussian filtering is set at 2 kHz, this would be 600 μs).

Events considered in the closed time distribution included all 50% threshold crossings and therefore included more events than the open time distributions. The amplitude, open time, and closed time data were binned and fit using the Levenberg-Marquardt algorithm with multiple Gaussian distributions or multiple exponentials to determine the mean event amplitude, mean open time, and mean closed time.

RESULTS

Light Activates Unitary Channel Currents of Two Distinct Amplitudes

In the dark, a cell-attached patch from the light-sensitive lobe of a *Limulus* ventral photoreceptor typically showed no channel activity. The response to light had an early phase characterized by high channel activity followed by a late phase with reduced channel activity, a pattern that resembles the macroscopic response (Baciga-lupo and Lisman, 1983, 1984). During illumination, there were both large and small channel events (Fig. 1 *A*). Previous work showed that the large events cannot be induced by depolarization in the dark, implying that the large events are induced by light rather than by the depolarization produced by light. Fig. 1 *B* shows that this is also true for small events.

Since many channel openings were very brief (a millisecond or less), it was important to establish that the small events were really a separate type of event rather than attenuated large events. Fig. 2 shows the probability density histogram of the current for all data points in a 75-s period with the number of observations on the ordinate displayed on a logarithmic scale. The data have been fit with the sum of three Gaussian distributions. The first and largest amplitude Gaussian is centered at zero current and describes the distribution of the baseline points. The two additional Gaussians that describe channel activity have peaks at -0.678 ± 0.203 and -1.417 ± 0.497 pA (mean ± SD). The triple Gaussian fit was significantly better than that with a double Gaussian (χ^2/degrees of freedom: 0.49 [triple Gaussian] vs. 2.1 [double

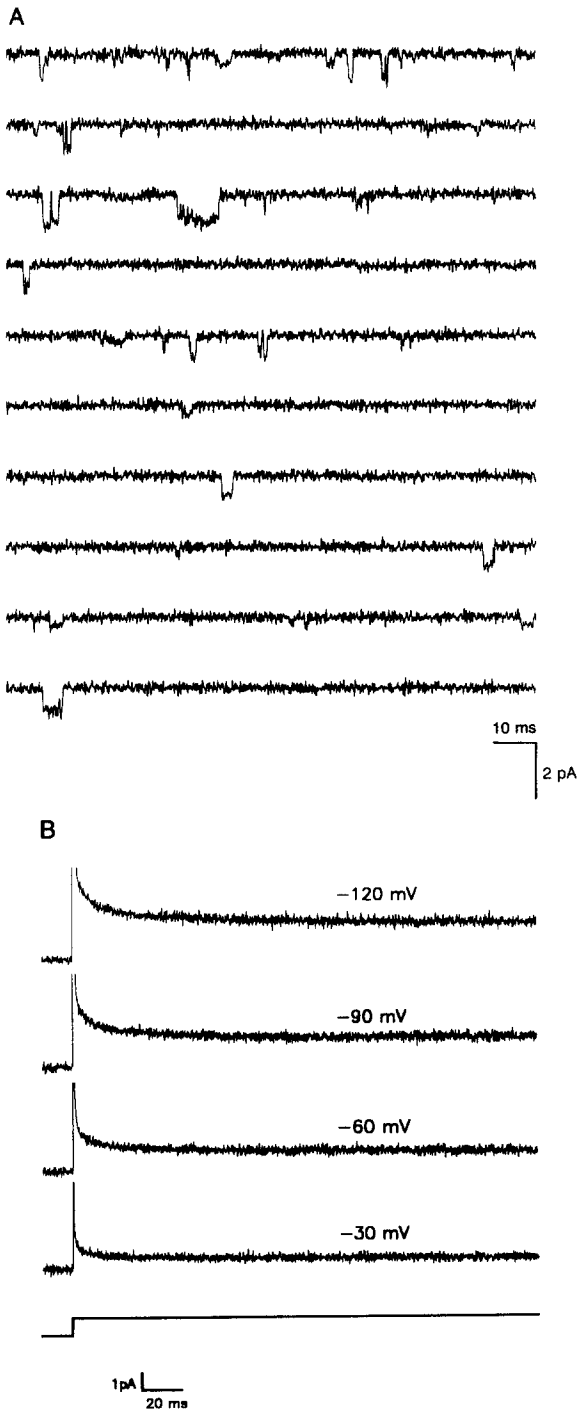

FIGURE 1. Two sizes of channel events are evoked by light and cannot be activated by depolarization in the dark. (*A*) Consecutive traces during illumination of a cell-attached patch (bandwidth is 2,000 Hz DC, set at playback) with no voltage applied to the pipette (at this level of illumination, the absolute membrane potential of the cell is ~ -30 mV). Events of two sizes are seen. Light stimulus is $\sim 10^{14}$ photons cm^{-2} s^{-1} at the level of the preparation. (*B*) In the dark, depolarizing steps in increments of 30 mV were applied to the pipette (up to 120 mV) from resting potential (~ -50 mV). The applied pipette potential is shown above each trace. No channel events were observed at any of these voltages. Top traces are the patch current; bottom trace is the voltage monitor. After each voltage step the voltage returned to zero.

Gaussian]). Thus, the data are best accounted for by more than a single population of channel events and most likely two populations.

The size distribution of single-channel events was further characterized by detecting events that were larger than a criterion threshold and open long enough for the

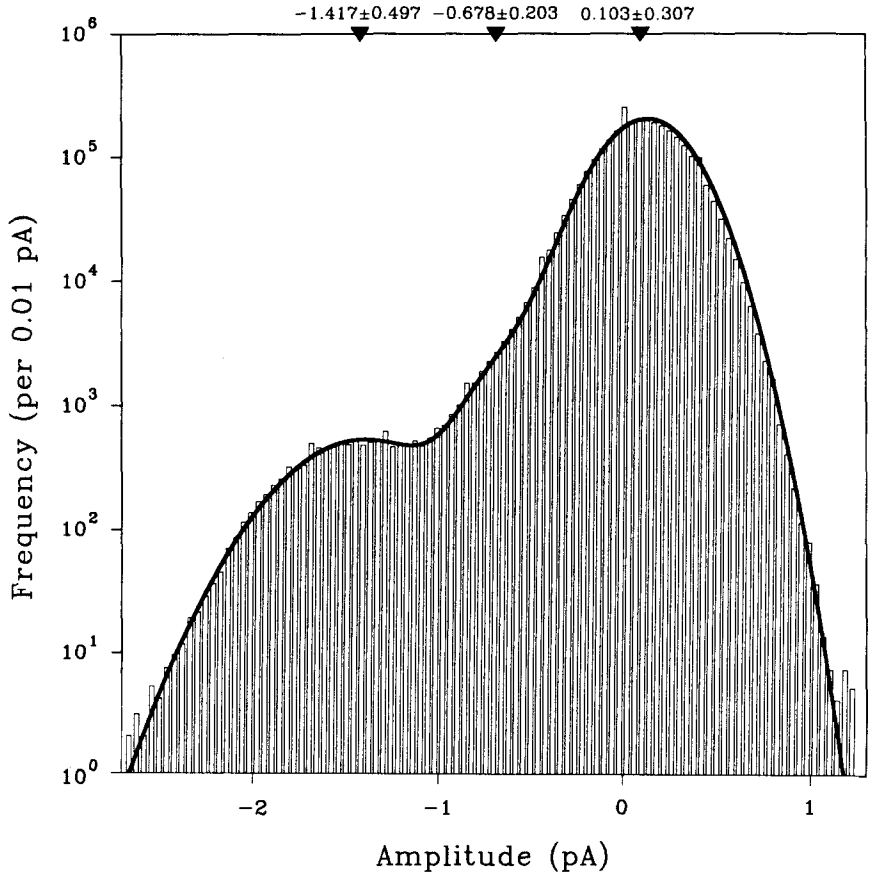

FIGURE 2. Raw probability density histogram of the digitized patch clamp current recorded during the steady-state phase of the light response. Data were digitized during a 75-s period of illumination at 10 kHz; the digital Gaussian filter resulted in a final bandwidth of 2.37 kHz. Amplitude histogram is displayed as the logarithm of the number of samples. These data can be best fit by the sum of three Gaussians. The largest Gaussian is the baseline noise. The fit parameters are the weight factor (W), the midpoint (mean), and standard deviation (SD): W-1 348.75, mean-1 = 0.103, SD-1 = 0.307; W-2 = 12.46, mean-2 = −0.678, SD-2 = 0.203; W-3 = 30.06, mean-3 = −1.417, SD-3 = 0.497. The data are from the same patch as Fig. 1.

current to settle (see Materials and Methods). Fig. 3 shows an amplitude distribution of such events. The histogram was adequately fit with the sum of two Gaussians, −0.62 ± 0.16 and −1.47 ± 0.33 pA (mean ± SD). Recordings from 15 of 20 patches had substantial numbers of both large and small events. In five patches one of the

event classes occurred too infrequently to be fit by a Gaussian; one of these patches had predominately small events, whereas four patches had predominately large events. In some patches there were small numbers of even larger events (≈58 pS) that were seen most frequently at early times during the response to light. Such events were rare or absent during the steady-state phase of the response in most patches, and were not characterized further.

The current–voltage relationships for small and large events from the same patch are shown in Fig. 4. The slope conductances are 15 and 40 pS, respectively. For 15 patches studied, the values were 14.9 ± 3.1 (mean ± SD; n = 15) and 39.7 ± 3.8 (n = 15). The reversal potential for both types of discrete current events is the same; 40 mV depolarized from the membrane potential of the illuminated cell (~ −30 mV). This implies that the absolute value of the reversal potential is about +10 mV, in agreement with previous work on the large events (Bacigalupo and Lisman, 1984)

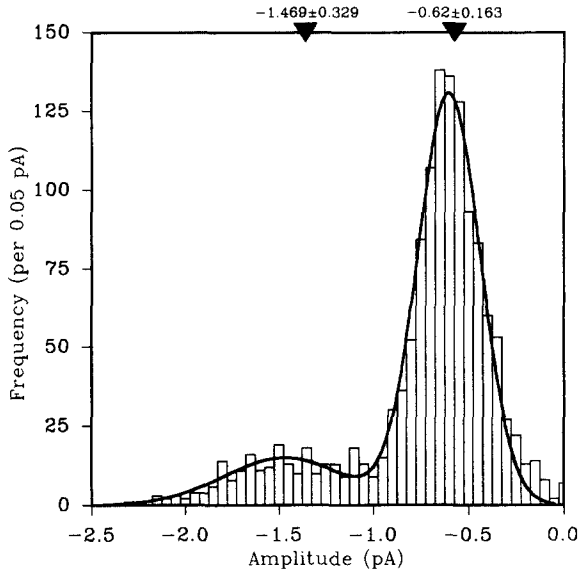

FIGURE 3. Histogram for the idealized events whose amplitude was larger than threshold (0.31 pA, ~50% of the small events) and longer than 600 μs. From the same experiment as Fig. 2. Two peaks can be easily distinguished and a double Gaussian distribution (χ^2/degrees of freedom = 3.8) was fitted with peaks at −0.620 ± 0.163 (mean ± SD) and −1.469 ± 0.330 pA.

and the macroscopic conductance (Millecchia and Mauro, 1969). In most cells the current–voltage curve of the open channel demonstrated some outward rectification when the patch was depolarized >90 mV during illumination. This rectification was not observed in all patches; when present it was always greater for the small events than for large ones.

Kinetic Properties of the Light-activated Unitary Events

Both large and small events sometimes have brief closures (<1 ms) that are distinguishable from the long closed periods which separate other openings. The distinction between such closures is demonstrated by closed time histograms that are fit by a combination of a very brief (<1 ms) and a much longer exponential time constant (Fig. 5). Brief closures of this kind are typically referred to as flickering. It

should be noted that flickering closures are relatively rare. For the patch illustrated in Fig. 5, the area under the fast component of the curve is only ~20% of the total area, indicating that most events do not contain a detectable flickering closure.

The histogram of open durations for the large and small events at zero applied pipette potential under steady illumination is shown in Fig. 6. In making the measurements of open time, brief closings due to flickering were ignored because it was clear that many such flickering events would go undetected. As a result the open time distributions should technically be considered a burst time distribution. The open time histograms for both large and small events were adequately fit by a single exponential, consistent with a single open state. The mean open time for large events was 2.38 ± 0.73 ms, n = 15 (mean ± SD, for n patches), somewhat longer than for the small events (1.34 ± 0.49 ms; n = 15).

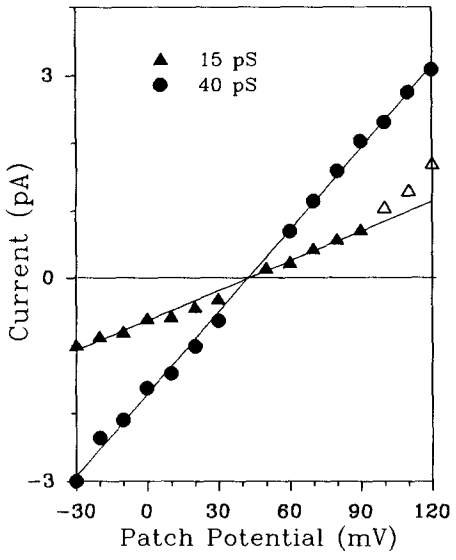

FIGURE 4. Current-voltage relations for the large conductance (●) and the small conductance (△, ▲) light-activated events. The voltage values on the abscissa correspond to the voltages applied to the pipette during the application of a prolonged light. Zero voltage is the resting membrane potential of an illuminated cell (~ −30 mV). Each point represents the peak of a Gaussian fit of the data at the corresponding voltage as in Fig. 3. The two sets of points shown by filled symbols were fitted by linear regression. Slopes conductances were 40 and 15 pS. At very positive potentials the small events deviate from linearity. At 120 mV this deviation is significant at $P < 0.05$. These points were not included in fitting the slope.

The large light-activated event has a probability of being open that is insensitive to voltage at negative voltages and that increases dramatically at positive voltages (Bacigalupo et al., 1986), consistent with the voltage-dependence of the macroscopic light-activated conductance (Millecchia and Mauro, 1969). As shown in Fig. 7, the voltage dependence of the probability of being open for the small event is similar to that of the large event. The data in Fig. 7 are from a patch that contained only one channel as shown by subsequent analysis below (see below). Previous work on large conductance events (Bacigalupo et al., 1986) showed that the mean open time increases at positive voltages and that this is the major reason for the voltage-dependent increase in probability of being open. Although we have not examined this question in detail for the small event, the data indicate that the mean open time of the small event is also larger at positive voltages. For example, in the patch of Fig.

8, at zero applied pipette potential, the mean open times for the large and small events are 2.2 and 1.3 ms, respectively, while at a pipette potential of +100 mV they are 10.7 and 8.3 ms.

Large and Small Events Are Due to Two Different Conductance States of the Light-activated Channel

Large and small events might be produced by two types of light-activated channels; alternatively, they might be due to different conductance states of the same channel type. We addressed this issue using two different tests. In the first test we examine the

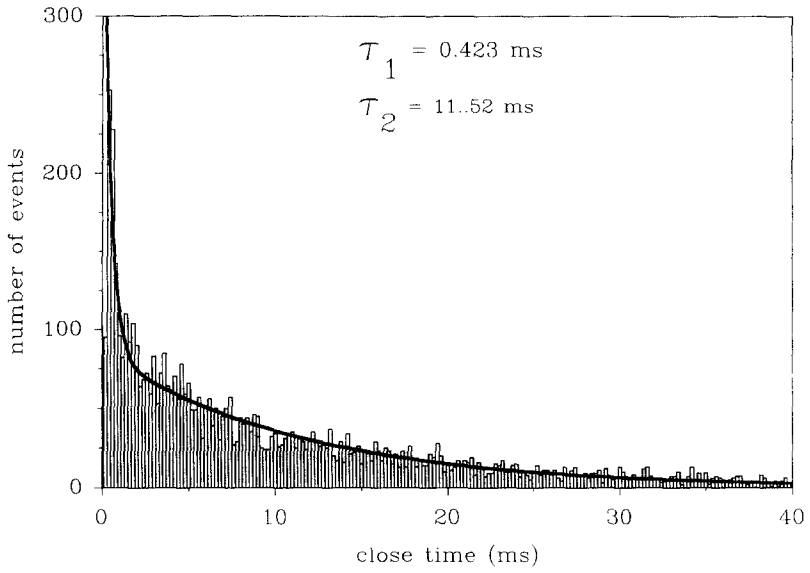

FIGURE 5. Distribution for all closed times in the recording at zero applied voltage. This was calculated from the time between successive threshold crossings (0.35 pA) for either size events. Two exponentials were fitted with time constants 0.423 and 11.52 ms. The distribution includes events that were not open sufficiently long to determine which conductance level was reached, but long enough to define the end of a closing (see Materials and Methods). This included 693 15-pS events, 180 40-pS events, and 4,413 events that crossed threshold but were open too short to determine the conductance level. The data are from the same patch as Fig. 1.

issue of overlap of large and small events. Failure to find overlap would argue for a single type of channel with multiple conductance states. This test was most critical at positive voltages for two reasons. First, at positive voltages, as just shown, the probability of a channel being open is high. Thus, if different conductance states were independent, a reasonable number of overlaps would be expected. Second, because the mean open time is quite long at positive voltages, there is little chance that overlapping events would be missed due to limited frequency response. If the large and small events are due to two different ion channels that open independently, the probability that both channels are open simultaneously is the product of the

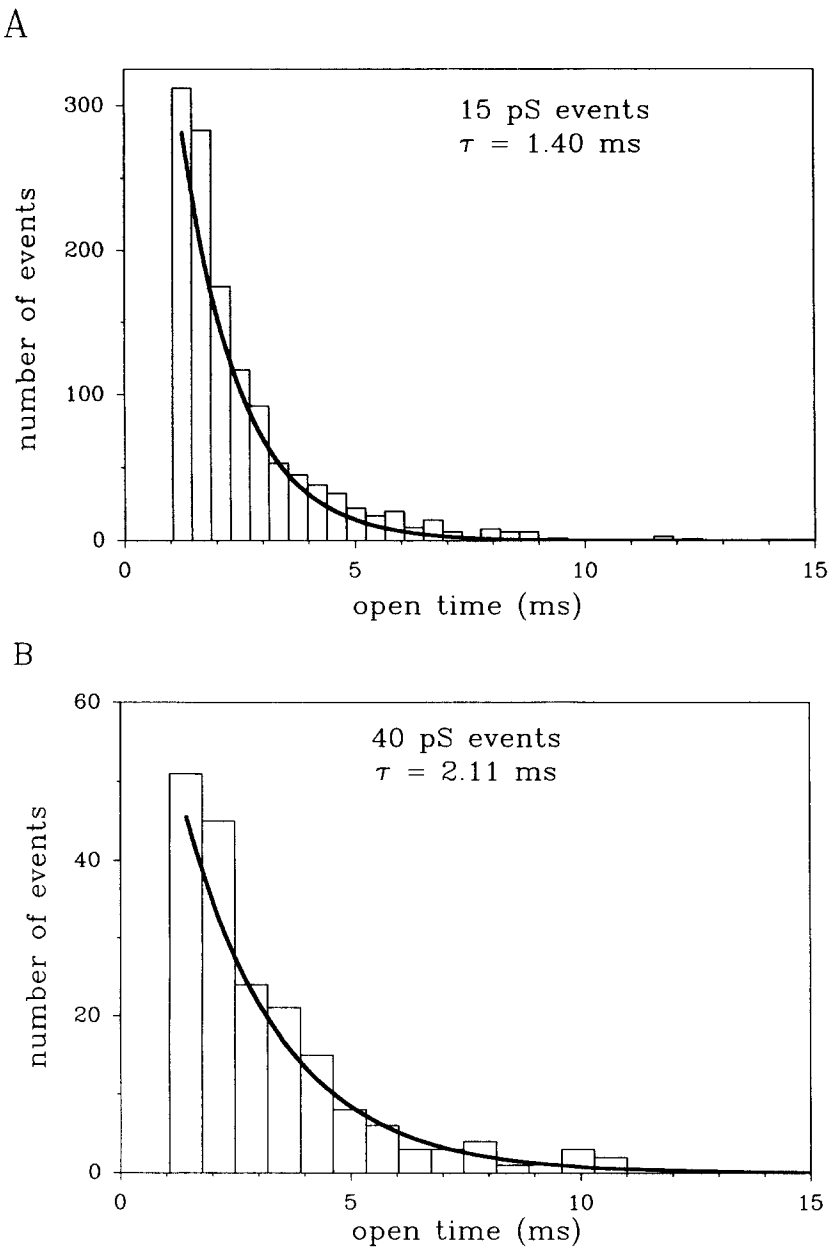

FIGURE 6. Distribution of open times for the two sizes of events at zero applied patch potential during steady-state illumination. (*A*) Open time distribution for the 15-pS events. One exponential was fit to the data with a time constant of 1.40 ms. (*B*) Open time distribution for the 40-pS events fit with one exponential, time constant 2.11 ms. The data are from the same patch as Fig. 1.

probability of the small event being open times the probability of the large event being open. In Fig. 7, when the patch was depolarized by +120 mV, the probability of being open for the small and large events was 0.24 and 0.38, respectively, giving a probability of overlap of 0.09. Given that the mean open times of the large and small events were 11.1 and 8.8 ms, respectively, the dwell time of a randomly occurring overlapping event would be 4.9 ms; such an event would be easily observed in our recording system. From the predicted probability of overlap (0.09) and the predicted dwell time of overlap, we would expect 367 randomly occurring overlapping events in a 20-s stretch of data; however, no overlaps were observed. Similar observations were made at other positive voltages. In the patch of Fig. 8 *A*, when depolarized by +100 mV, the probability of being open for the small and large events was 0.27 and 0.075, respectively, giving a probability of both being open of 0.02. In this patch the dwell

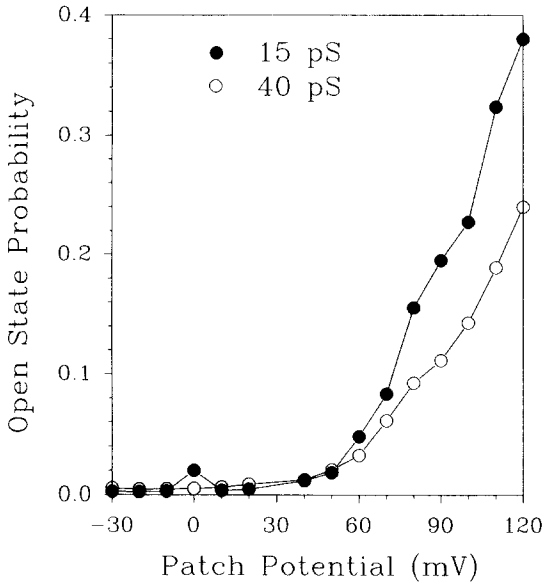

FIGURE 7. The open-state probability of large and small events is voltage dependent. The probability of being open was determined by the duration spent in a given level divided by the total time of the measurement. At zero applied voltage the membrane potential is ~−30 mV. (○) 40-pS events; (●) 15-pS events. Each point represents the open-state probability calculated from the integral of at least 50 events of each size. The data are from the same patch as Fig. 1.

time of a randomly occurring overlapping event is 4.7 ms, and we would expect 123 randomly occurring overlapping events. Again, in a 29-s stretch of data no overlaps were observed. In this patch, the observed probability of being open at the level of 15 + 40 pS was 0.0055, however, all of these events were due to rare 58-pS events which made direct transitions to and from baseline. Most patches contained multiple channels. In such patches superposed large and small events were, of course, common.

A second test for multiple conductance states is whether there are direct transitions between current levels. Transitions are observed relatively frequently at positive voltages, where the probability of being open is high, and less frequently at negative voltages. Within each of three traces in Fig. 8 *A* there are several transitions between current levels that do not involve a transition back to baseline. Because of the low

frequency of transitions it was important to do statistical analysis to determine whether these represented true transitions or were only apparent transitions caused by two independent sequential events. Apparent transitions could occur when one event ends at nearly the same time that the other begins; because of limitations in the frequency response of the recording system, this would appear to fuse into a single event with two levels. In the experiment of Fig. 8 *B*, there was a total of 375 events, 18 of which showed direct transitions between current levels. These observations were

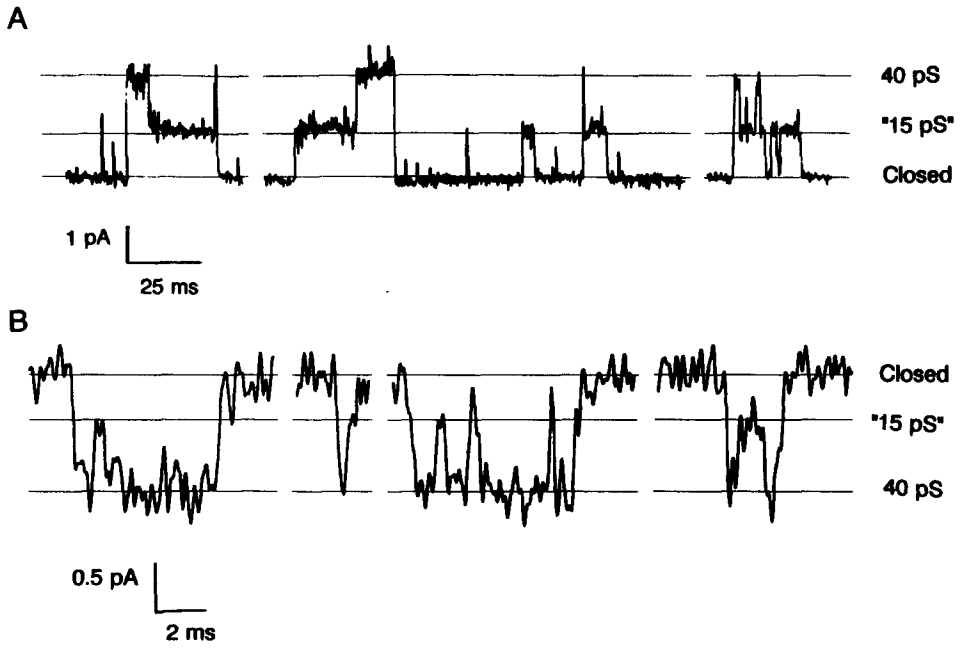

FIGURE 8. Direct transitions between conductance levels (*A*) A series of transitions in each of three selected traces from a patch depolarized by 100 mV (driving force ≈ 60 mV). Note that because of the outward rectification of the small conductance, the "15 pS" events are about half the size of the "40 pS" events. The high frequency of transitions between event levels in such short periods indicates that these are substates of a single ion channel (see text). (*B*) Transitions observed at zero applied patch potential (driving force ≈ −40 mV) in the same patch as *A*. Transitions occur much less frequently, owing to the much lower open-state probability at this patch potential. Bandwidth in each is DC to 2,000 Hz. Lines indicate zero conductance level (closed channel) and the "15 pS" and "40 pS" states in this patch.

confirmed by reexamination at 10 kHz frequency response. Of such transitions, 8 went from the large conductance to the small conductance level and 10 from the small to the large conductance level, therefore not showing any preference of one type of transition over the other. If large and small events are independent, the predicted frequency of apparent transitions from a large event to a small event can be calculated from the rate of large events times the probability that a small event will begin after the end of the large event within the time that a closing to baseline cannot

be resolved. This probability is the rate of the small events times the time resolution. A flickering closure of a large channel followed by an opening of a small channel would not generate the kind of transition we observed because it would be rapidly followed by a transition to the sum of the large and small conductance levels at the end of the flickering closure. In calculating the rate of expected transitions it was therefore appropriate to use the rate of events without counting the openings due to flickering (i.e., the rate of bursts).

The time resolution was determined by simulating impulse responses through a Gaussian filter with noise and determining the separation in time needed between two events to determine that they are independent. This value is ~ 100 μs for a Gaussian filter with a cutoff at 2 kHz. In the patch of Fig. 1, for data at zero applied pipette potential, the frequency of small events was 4.4 s^{-1} and the frequency of large events was 2.5 s^{-1}. Using these values, the predicted frequency of apparent transitions is $1.1 \cdot 10^{-3}$ s^{-1}, the observed frequency is much greater, 0.12 s^{-1}. In a total of five patches, at zero applied patch potential, in which this analysis was done, we found an average of 3.7% of the events contained a transition to the other sized event (range: from 2.1% to 7.6%), all of these much greater than the predicted number of transitions. We conclude, using a χ^2 test, that the number of observed transitions is significantly greater than the predicted number of "false" transitions ($P < 0.005$, $n = 5$). Fig. 8 *A* shows several current traces during illumination of a patch depolarized by +100 mV and containing only a single light-activated channel. Such transitions were common. The same statistical analysis was also done for data obtained at positive voltages where we also observed a statistically significant frequency of true transitions (1.3 ± 0.83 s^{-1}; $P < 0.001$, $n = 4$).

In predicting the frequency of apparent transitions, we have assumed that large and small events occur randomly in time. As will be shown in the next section, this is not the case; large and small events tend to occur in runs having durations on the order of several hundred milliseconds. This grouping of events of the same size makes it even more unlikely that the observed transitions between large and small events is due to the closure of one type of channel concurrent with the opening of the other. The calculations of apparent transitions given above should therefore be considered worst case calculations. The fact that even under these worst case conditions the observed transitions cannot be accounted for by sequential events in two different channels emphasizes the conclusion that the transitions are real and that large and small events are due to substates of the same channel.

Modes of the Channel during Illumination

During examination of channel activity evoked by prolonged illumination we noted that events of a given size appeared to occur in groups. This was only observed in patches that had only one channel as evidenced by the absence of overlap when the probability of being open is high at positive voltages. This grouping sometimes occurred over periods of several hundred milliseconds, a period much longer than the channel open time and much longer than the fast or bursting time constant of the closed time histogram. To illustrate this phenomenon, we constructed plots of the type shown in Fig. 9 *A* from a patch hyperpolarized by 30 mV. The ordinate in this plot represents the number of consecutive events of the same conductance. Positive deflections represent openings to the high conductance state; negative deflections

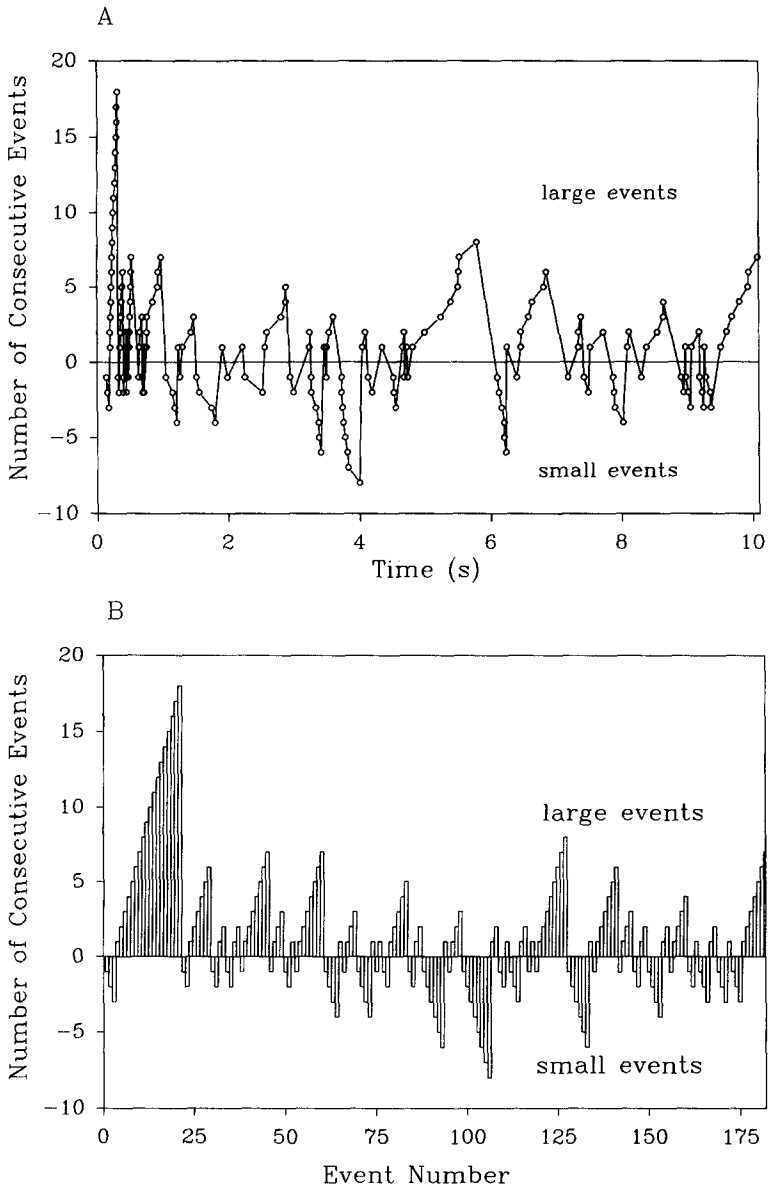

FIGURE 9. Conductance modes of the light-activated channel activity. (*A*) Plot of the number of consecutive events having the same conductance level versus time. Positive points: large events. Negative points: small events. There were 145 consecutive events. Patch potential hyperpolarized by 30 mV. Zero time is onset of light, but events in the first 100 ms omitted. (*B*) The same data as in *A*, but plotted as a function of total event number.

represent openings to the low conductance state. The abscissa in Fig. 9 *A* represents the events plotted as a function of time; the abscissa in Fig. 9 *B* represents the event number, ordered according to their occurrence during the response to light. In counting channel openings, flickering events (<0.8 ms) were ignored. Fig. 9 *A* shows

that clustering occurred over long periods of time. In this patch, for instance, there was one period of 980 ms during which there were eight sequential openings of the large conductance state without a single opening to the small one. Similarly, there was a period of 270 ms in which there were eight sequential opening to the small state without any openings to the large state. This clustering is observed at both hyperpolarizing (data shown) and depolarizing voltages (100 mV).

To determine whether such sequences might arise randomly we analyzed the data according to the statistics of "runs" (Mood and Graybill, 1963). A run is a group of events of a given kind, with no interposed events of any other kind. According to this theory, the number of runs expected to occur randomly (μ) is calculated by

$$\mu = \frac{2n_S \cdot n_L}{n_S + n_L} + 1$$

where n_S is the number of small events and n_L is the number of large events. The standard deviation of the expected number of runs is determined by

$$\sigma = \sqrt{\frac{2n_S \cdot n_L(2n_S \cdot n_L - n_S - n_L)}{(n_S + n_L)^2(n_S + n_L - 1)}}$$

The likelihood that the number of observed runs should differ from the number of predicted runs can be evaluated from the normal deviate test comparing the difference between the observed and predicted number of random runs. For the experiment shown in Fig. 9, there were 62 runs, 77 small events, and 109 large ones; the calculated number of randomly occurring runs 91.25 ± 6.6 (mean ± SD) does not satisfactorily predict our observation ($P < 0.0001$). It is important to emphasize that flickering closures were ignored in determining these numbers. In a second patch there were 398 events and 90 runs; the calculated number of runs was 193 ± 9.93 (mean ± SD) which also does not satisfy the null hypothesis ($P < 0.00001$). These results indicate that the grouping into runs cannot be accounted for by random interspersing of independent large and small events. Similar analysis was done in three other patches and these patches demonstrate a similar statistical significance of the "modes" ($P < 0.0001$). Thus, we conclude from this analysis that a single type of channel opens in modes preferentially to one or the other conductance state. Statistically significant runs were not observable in patches with many light-dependent channels.

During the early parts of the response (the first few hundred milliseconds) most patches showed many more large events than small ones, whereas during later parts of the response the relative proportion of small events was much greater. To illustrate the relative contribution of large and small events during different parts of the response to light, amplitude distributions of the events that occurred during the early phase of the response (first 400 ms) and the late part of the response (from 400 ms to the end of light) were constructed. An illustration of this is shown in Fig. 10 (the same patch as Fig. 1). Events that occurred before the end of the transient phase of the receptor potential were not counted. The figure shows that in the first period of the response the channel opened preferentially to the high conductance state, whereas during the latter part of the response the channel opened preferentially to the low

conductance state. Similar results were obtained in the eight other patches in which we had a large enough number of events to make this kind of histogram. These results indicate that the expression of the different modes of the light-activated channel is not random, but depends upon the physiological state of the photoreceptor.

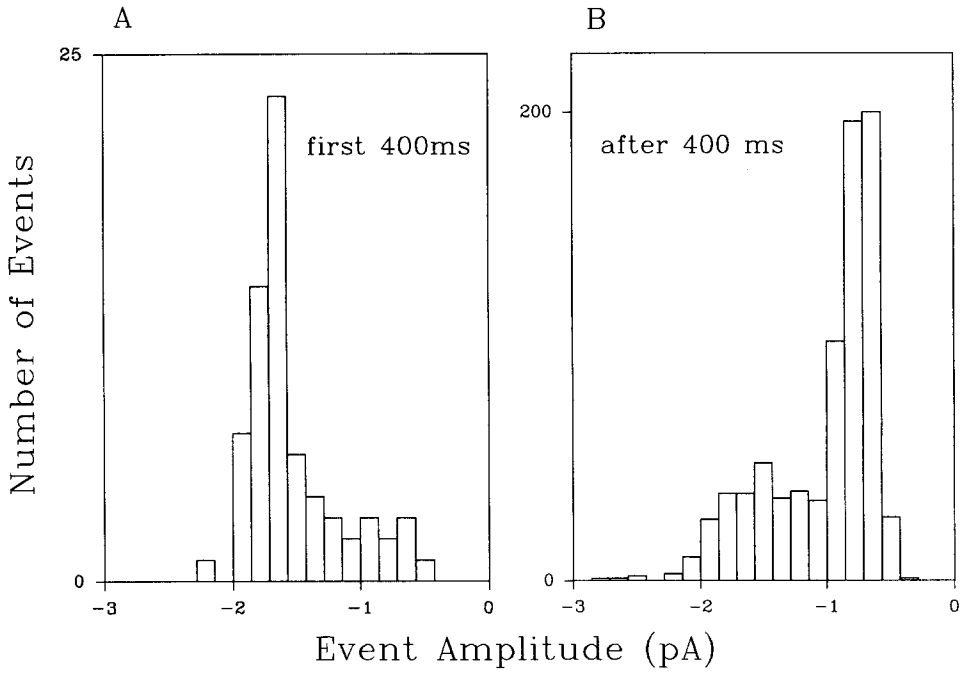

FIGURE 10. The preferred conductance state changes with time after the onset of illumination at zero applied patch potential. Amplitude distributions were constructed from the response to one illumination in the same manner as Fig. 3 of the events during the early part of the light response (*A*, first 400 ms or first 70 events; none of which occurred during the time the membrane potential was rapidly changing potential in this patch) and during the latter part of the response (*B*, after 400 ms or events 71–800). There were no superimpositions of events in this stretch of data. Same patch as in Fig. 1.

DISCUSSION

Cell-attached recordings from *Limulus* ventral photoreceptors show that there are light-activated single-channel events of two different sizes. We present here several lines of evidence indicating that large and small events are due to distinct states of the same channel rather than to two different channel proteins. Large and small events have a similar reversal potential and a similar dependence of open probability on voltage. These similarities suggest that large and small events are generated by the same channel, but do not prove it. The observation that large and small events occur in long runs (Fig. 9) demonstrates that the large and small events are generated by a coupled mechanism. The simplest explanation of these runs is that

both events are generated by a single channel that changes modes, but there are alternative explanations. Definitive evidence that large and small events are generated by the same channel comes from the observation of direct transitions between the two conductance levels at positive voltages and the failure to observe superposition of the two types of events. Statistical analysis of such transitions excludes the possibility that they arise from two different channels, one of which opens while the other closes just at the right time to give the false appearance a direct transition between levels. Thus, the data support the conclusion that the *Limulus* light-activated channel has at least two conductance states.

The occurrence of multiple conductance states has been demonstrated for many different types of channels (Fox, 1987). In some cases, the channel dwells most often in one state, occasionally visiting substates. This is the case for the acetylcholine-activated channel (Auerbach and Sachs, 1983; Morris and Montpetit, 1986), the Ca-activated potassium channel (Vergara, 1983) and the sodium channel (Patlak, 1988). In other channel types, the channel activity is more evenly distributed among its conductance states. This is the case for the glutamate-activated channel (Cull-Candy and Usowicz, 1987; Jahr and Stevens, 1987) and the light-dependent channel from vertebrate photoreceptors (Hanke et al., 1988; Haynes and Yau, 1990). For the *Limulus* light-activated channel, both states are expressed with roughly equal frequency in some cells, although not in all cells. What is very unusual about the light-activated channel is how infrequently transitions between these states occur, and this is especially true at negative voltages where most events open to one or the other conductance state and then close. This low probability of transition may be an expression of the fact that the channel switches slowly between modes that determine which conductance state is expressed.

During the steady-state phase of the response to light, the channel slowly switches back and forth between modes (Fig. 9). While in a given mode, the channel opens repeatedly to a given conductance level. Statistical analysis of these runs shows that they cannot be accounted for by random events. We do not yet have good numbers for the lifetime of each mode, but it is clear that this lifetime is on the order of a few hundred milliseconds, two orders of magnitude larger than the channel lifetime. Previous work on other channels has exhibited modes of gating behavior (Hess et al., 1984; Patlak and Ortiz, 1986); the *Limulus* light-activated channel differs in that the mode affects conductance properties in addition to gating properties.

It has recently been proposed that there may be two separate second messenger pathways leading to activation of inward current in *Limulus* photoreceptors, one involving calcium ions (released by inositol trisphosphatase), the other involving another second messenger (Frank and Fein, 1991). It has further been suggested (Nagy and Stieve, 1990) that there are 10- and 29-pS single-channel events, that these are due to two independent types of light-dependent channel (but no evidence against these being substates of the same channel was presented), and that these might be activated by different second messengers. The work presented here is not consistent with this view; insofar as our evidence suggests that there is only one kind of light-dependent channel (with different substates), our data provide no support for two separate transduction pathways. We furthermore considered the possibility that there are two second messengers that can affect the same channel and determine

which conductance state is expressed. In particular, the modal oscillations of the light-dependent channel (Fig. 9) might, in theory, reflect oscillations of one or more second messengers. While we cannot rule out this possibility, it seems unlikely given that the modal behavior is not observed in patches with multiple channels. If oscillations of second messengers were involved, different channels in the same patch, which would be exposed to the same second messenger oscillations, ought to change their modes together, contrary to what is found.

Some comments are necessary regarding the discrepancy between the sizes of the single-channel conductances reported previously (Bacigalupo et al., 1986) of 39.2 ± 2.8 pS (mean ± SEM, $n = 5$) compared to those reported by Nagy and Stieve (1990) of 28.7 ± 3.4 pS. Nagy and Stieve (1990) argue that these differences might be due to the mild sonication procedure employed to enhance seal formation by Bacigalupo et al. (1986). This cannot be the source of the discrepancy since the single-channel conductances found in the work reported here, which did not use the sonication procedure, is in agreement with the conductance reported in previous work using this procedure. The discrepancy may, however, be related to differences in how reversal potential was measured. Nagy and Stieve (1990) measured only inward currents and determined the reversal potential by extrapolation over a large voltage range. Bacigalupo et al. (1986) as well as the work presented here (see Fig. 4) used a more accurate interpolation procedure using currents on both sides of the reversal potential. A related issue is whether the channels studied by Nagy and Stieve are somehow different than those reported by Bacigalupo et al. (1986) because of the differences in the latencies of channel activity after the onset of light, as suggested by Nagy and Stieve (1990). Examination of records from both laboratories, however, reveals them to be quite similar. In both, a positive deflection in the current trace occurs within 20 ms after the onset of bright illumination, but significantly preceding any light-dependent channel activity. This positive deflection is due to the onset of the macroscopic receptor potential and is generated through a capacitatively coupled transient. Channel activity in the patch is thus delayed by several milliseconds in data presented from both laboratories. For possible causes of this delay see Bacigalupo et al. (1986).

Functional Significance of Subconductance States

In general, the mechanism and function of subconductance states and channel modes have been unclear. In some chemically activated channels, the expression of conductance states depends on the agonist used (Cull-Candy and Usowicz, 1987) and on agonist concentration (Takeda and Trautwein, 1984), but the functional significance of this is not understood. A cellular function for substates in the *Limulus* light-dependent channel is suggested by the observation that during early periods of the response to light, the large conductance state is preferentially expressed whereas during the later periods, the small conductance state is preferentially expressed (Fig. 10). This can be related to macroscopic properties of the light response. Photoreceptors not only are excited by light, but also are adapted when illumination levels are high. Adaptation causes a reduction in gain that occurs with a delay after the onset of illumination (Lisman and Brown, 1975); because of this gain reduction the light-induced conductance is initially large but then decays to a much smaller value within

a few hundred milliseconds. In a second phase of adaptation, the conductance falls further over subsequent seconds until finally a steady state is achieved (Leonard and Lisman, 1981). The change in the preferred state of the light-activated channel described here (Fig. 10) is likely to contribute to the later phases of the adaptation process. Channel openings to the small conductance state not only allow a smaller current to flow, but the current flows for a shorter time (Fig. 6); we estimate that the charge-flow per opening is on the average at least fourfold less for the small channel than for the large one. Thus changes in the relative expression of large and small conductance states (Fig. 10) can have a significant impact on the current flowing into the cell.

Several important questions about the expression of different conductance states remain unanswered. On the basis of the present work we cannot give a precise definition of "mode." For instance, it is unclear whether a channel in a given mode always opens to one conductance state or merely prefers that conductance state. A second question concerns the number of conductance states. The fact that the 40 pS conductance state is preferentially expressed at early parts of the response to light raises the possibility that yet higher conductance states may be expressed during the first few hundred milliseconds of the response, a period that we have not studied because of the rapidly changing voltage. This is an important part of the response since much of the adaptation occurs during this time. To study this period it will be necessary to voltage-clamp the cell. Finally, it is of interest to know the mechanism underlying mode changes. One possibility is that mode changes may involve a cycle of phosphorylation and dephosphorylation of the channel, but other possibilities can in no way be excluded.

We would like to thank Dr. Bertil Hille for his suggestion on how to plot the data in Fig. 9, Dr. Raul Espinosa for helpful discussions, Drs. Gordon Fain and Irwin Levitan for comments on the manuscript, and Mr. Taoufik Sadat for computer assistance.

This work was supported by National Institutes of Health grant EY01496 to Dr. Lisman and National Science Foundation grants BNS-8812455 to Dr. Johnson and INT-8610625 to Dr. Bacigalupo.

Original version received 28 October 1989 and accepted version received 13 December 1990.

REFERENCES

Auerbach, A., and F. Sachs. 1982. Flickering of a nicotinic ion channel to a subconductance state. *Biophysical Journal.* 42:1–10.

Bacigalupo, J., K. Chinn, and J. E. Lisman. 1986. Ion channels activated by light in *Limulus* ventral photoreceptors. *Journal of General Physiology.* 87:73–89.

Bacigalupo, J., E. C. Johnson, P. Robinson, and J. E. Lisman. 1990. Second messengers in invertebrate phototransduction. *In* Transduction in Biological Systems, C. Hidalgo, J. Bacigalupo, E. Jaimovich, and J. Vergara, editors. Plenum Publishing Corp., New York. 27–45.

Bacigalupo, J., E. C. Johnson, C. Vergara, and J. E. Lisman. 1991. Cyclic GMP opens light-dependent channels in excised patches of *Limulus* ventral photoreceptors. *Biophysical Journal.* 59:530*a*. (Abstr.)

Bacigalupo, J., and J. E. Lisman. 1983. Single-channel currents activated by light in *Limulus* ventral photoreceptors. *Nature.* 304:268–270.

Bacigalupo, J., and J. E. Lisman. 1984. Light-activated channels in *Limulus* ventral photoreceptors. *Biophysical Journal.* 45:3–5.

Bacigalupo, J., J. E. Lisman, and E. C. Johnson. 1987. A low conductance light-dependent channel observed in cell attached and excised patches of *Limulus* ventral photoreceptors. *Biophysical Journal.* 55:39*a*. (Abstr.)

Cull-Candy, S. G., and M. M. Usowicz. 1987. Multiple-conductance channels activated by excitatory amino acids in cerebellar neurons. *Nature.* 325:525–528.

Fox, J. A. 1987. Ion channel subconductance states. *Journal of Membrane Biology.* 97:1–8.

Frank, T. M., and A. Fein. 1991. The role of the inositol phosphate cascade in visual excitation of invertebrate microvillar photoreceptors. *Journal of General Physiology.* 97:697–723.

Hanke, W., N. J. Cook, and U. B. Kaupp. 1988. cGMP-dependent channel protein from photoreceptor membranes: single-channel activity of the purified and reconstituted protein. *Proceedings of the National Academy of Sciences.* 85:94–98.

Haynes, L., and K.-W. Yau. 1990. The cyclic GMP-Gated channels of rod and cone photoreceptors. *In* Transduction in Biological Systems. C. Hidalgo, J. Bacigalupo, E. Jaimovich and J. Vergara, editors. Plenum Publishing Corp., New York. 47–73.

Hess, P., J. B. Lansmann, and R. W. Tsien. 1984. Different modes of Ca channel gating behaviour favoured by dihydropyridine Ca agonists and antagonists. *Nature.* 311:538–544.

Johnson, E. C., P. R. Robinson, and J. E. Lisman. 1986. Cyclic GMP is involved in the excitation of invertebrate photoreceptors. *Nature.* 324:468–470.

Jahr, C. E., and C. F. Stevens. 1987. Glutamate activates multiple single channel conductances in hippocampal neurons. *Nature.* 325:522–525.

Leonard, R. J., and J. E. Lisman. 1981. Light modulates voltage-dependent potassium channels in *Limulus* ventral photoreceptors. *Science.* 212:1273–1275.

Lisman, J. E., and J. E. Brown. 1975. Light-induced changes of sensitivity in *Limulus* ventral photoreceptors. *Journal of General Physiology.* 66:473–488.

Lisman, J. E., E. C. Johnson, J. Bacigalupo, and C. Vergara. 1990. Alteration of conductance state of light dependent channel in *Limulus* ventral photoreceptor. *Biophysical Journal.* 57:366a. (Abstr.)

Millecchia, R., and A. Mauro. 1969. The ventral photoreceptor cells of *Limulus.* III. A voltage-clamp study. *Journal of General Physiology.* 54:331–351.

Mood, A. M., and F. A. Graybill. 1963. Introduction to the Theory of Statistics. McGraw-Hill Book Co., Inc. New York. 409–417.

Morris, C. E., and M. Monpetit. 1986. Multiple conductance states of the acetylcholine receptor channel complex. *Canadian Journal of Physiology and Pharmacology.* 64:347–355.

Nagy, K., and H. Stieve. 1990. Light-activated single channel currents in *Limulus* ventral nerve photoreceptors. *European Biophysics Journal.* 18:221–224.

Patlak, J. B. 1988. Sodium channel subconductance levels measured with a new variance-mean analysis. *Journal of General Physiology.* 92:413–430.

Patlak, J. B., and M. Ortiz. 1986. Two modes of gating during late Na^+ channel currents in frog sartorius muscle. *Journal of General Physiology.* 87:305–326.

Stern, J., K. Chinn, J. Bacigalupo, and J. Lisman. 1982. Distinct lobes in *Limulus* ventral photoreceptors. I. Functional and anatomical properties of lobes revealed by removal of glial cells. *Journal of General Physiology.* 80:825–837.

Takeda, K., and A. Trautmann. 1984. A patch-clamp study of the partial agonist actions of tubocurarine on rat myotubes. *Journal of Physiology.* 349:353–374.

Vergara, C. 1983. A characterization of the Ca-activated K-channel in planar lipid bilayers. Ph.D. thesis. Harvard University, Cambridge, MA.

Wong, F., B. W. Knight, and F. A. Dodge. 1982. Adapting bump model for ventral photoreceptors of *Limulus. Journal of General Physiology.* 79:1089–1113.